

Single-input Multiple-output Tunable Log-domain Current-mode Universal Filter

Pipat PROMMEE, Kobchai DEJHAN

Department of Telecommunications Engineering, Faculty of Engineering,
King Mongkut's Institute of Technology Ladkrabang, Bangkok 10520, Thailand

pipat@telecom.kmitl.ac.th

Abstract. *This paper describes the design of a current-mode single-input multiple-output (SIMO) universal filter based on the log-domain filtering concept. The circuit is a direct realization of a first-order differential equation for obtaining the lossy integrator circuit. Lossless integrators are realized by log-domain lossy integrators. The proposed filter comprises only two grounded capacitors and twenty-four transistors. This filter suits to operate in very high frequency (VHF) applications. The pole-frequency of the proposed filter can be controlled over five decade frequency range through bias currents. The pole- Q can be independently controlled with the pole-frequency. Non-ideal effects on the filter are studied in detail. A validated BJT model is used in the simulations operated by a single power supply, as low as 2.5 V. The simulation results using PSpice are included to confirm the good performances and are in agreement with the theory.*

Keywords

Log-domain filtering, very high frequency, low-voltage, electronically-controlled, universal filter.

1. Introduction

In 1979, Adams introduced a novel class of continuous-time filters called log-domain filters which externally are linear systems, yet internally are nonlinear [1]. This class originates from the companding concept (compress and expand) of log-domain circuits. Input linear current is initially converted to a compressed voltage, and then processed by the log-domain core block. The compressed output voltage is converted to a linear current to preserve the linear operation of the whole system. The compression and expansion of the corresponding signals are based on the logarithmic/exponential voltage-current relationship of a bipolar transistor. Log-domain circuits are useful building blocks for realizing high-performance current-mode analogue signal processing systems.

In 1993, Frey introduced a general method for synthesizing log-domain filters of arbitrary order using a state-space approach [2], [3]. Frey also presented a highly

modular technique for implementing such filters from a simple building block comprising a bipolar current mirror whose emitters are driven by complementary emitter followers. Log-domain filters based on instantaneous companding [4]–[7] and these circuits are both theoretical and technological interested, since they have potentially offered high-frequency operation, tunability, and extended dynamic range under low power supply voltages [8]–[20].

A biquadratic filter is a basic second-order function block for realizing high-order filter functions. The multi-function filter circuit based on a biquadratic function has been designed and developed for over four decade years [21]–[31]. The single output OTA (SO-OTA) was used in realizing the voltage-mode biquad filters based on a two-integrator loop structure in [22]. The circuit in [23] suffered from using a large number of OTAs. Other filters have been introduced based on multiple current output OTAs and grounded capacitors. The two-integrator loop current-mode filters based on lossless and lossy integrators (two OTAs and two grounded capacitors) were proposed in [24], [25]. The concept of component minimization for realizing the universal biquad filters has also been introduced. However, it cannot adjust pole- Q (Q_0) without affecting the pole-frequency (ω_0). Two-integrator loop structures using multiple current output OTAs and grounded capacitors have been introduced in [26], [27]. Summations of feedback of zeros to the rational function for realizing the filter were introduced in [28]–[31]; however, some circuits require too many active devices or excessive passive components and others cannot adjust the pole- Q without affecting the pole-frequency. The programmable zeros are obtained by either bias current or analogue switches. However, a performance limitation of the OTA including low bandwidth, high power supply and large die area can be observed.

Other active elements in the family of current conveyors including CCII [32–34], DVCC [35], DDCC [36] CCCII [37–40] and DXCCII [39] have been widely used for filter realization. However, the voltage and current tracking errors are the main problems of current conveyors. Active-only components based on OPAMP gain-bandwidth and OTAs have also been used in implementing the universal filter [42–43].

Unfortunately, several filters based on active building blocks (ABB) [21-43] are suitable for several megahertz range that they cannot operate in very high frequency applications. The narrow tunable range is a problem of ABB-based filter. Owing to log-domain filtering concept, it is including the following potential capabilities: low-voltage, high-frequency operation and wide electronic tunability. The above mentioned problems of ABB can be solved. In this paper, a high-frequency single-input multiple-output (SIMO) biquad universal filter is realized based on log-domain integrators loop. It is suitable for wireless systems [9] and high-frequency applications such as video signal processing, magnetic disk read channel, sensor signal conditioning [44]-[48]. The proposed circuit possesses the following features:

- 1) The configuration is realized by using minimum number of active and passive components.
- 2) Use of grounded capacitors, thus it is suitable for integration.
- 3) Orthogonal electronic tunability between ω_0 and Q_0 .
- 4) High-frequency operation is achieved based on the log-domain concept with wide electronic tunability and low-power supplies features.
- 5) High-output impedance, thus it enables interconnection to the succeeding current-mode circuits.

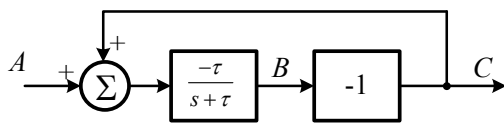


Fig. 1. Lossless integrator realized from a lossy integrator.

2. Theory and Principle

2.1 Lossless Integrator Realized by Lossy Integrator

Lossless and lossy integrators perform the same function as dependent building blocks, but a lossy integrator performs as a first order low-pass filter. A lossy integrator can be transformed to a lossless integrator or vice versa [19]. This paper uses the realization of a lossless integrator by transforming a lossy integrator. The inverting and non-inverting lossless integrators in Fig. 1 can easily be obtained by the transfer function at different nodes.

$$\frac{C(s)}{A(s)} = \frac{\tau}{s} \quad (1)$$

$$\frac{B(s)}{A(s)} = \frac{-\tau}{s} \quad (2)$$

2.2 Low-Pass Biquad Structure Realization

The inverting biquadratic low-pass (LP) function for synthesizing the system can generally be described by

$$\frac{Z(s)}{W(s)} = \frac{-AB}{s^2 + skA + AB}. \quad (3)$$

The above equation can be rewritten in terms of lossless integrators as follows:

$$Z(s) = [W(s) + Z(s)] \left(\frac{B}{s} \right) \left(\frac{-A}{s} \right) - kZ(s) \left(\frac{A}{s} \right). \quad (4)$$

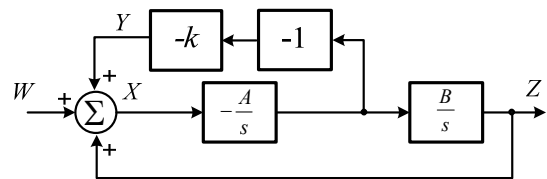


Fig. 2. Block diagram of a two-integrator loop filter.

Based on Fig. 2, other transfer functions of different nodes can, respectively, be obtained.

$$\frac{X(s)}{W(s)} = \frac{s^2}{s^2 + skA + AB}, \quad (5)$$

$$\frac{Y(s)}{W(s)} = \frac{-skA}{s^2 + skA + AB}. \quad (6)$$

2.3 Log-domain Lossy Integrator Based on Translinear BJT

Fig. 3(a) shows a log-domain filtering scheme based on a translinear type-B (balance) cell [49] which is called

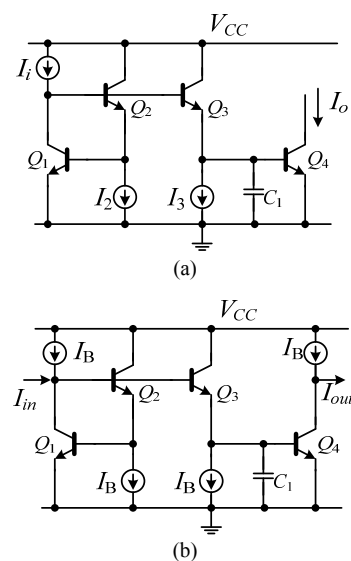


Fig. 3. Log-domain inverting lossy integrator (a) analytic structure, (b) practical structure.

a log-domain lossy integrator. Assuming that each transistor has an ideal exponential characteristic (base-current is neglected) and using Kirchhoff's current law (KCL), the base-emitter voltage relations can be written as

$$V_{be1} + V_{be2} - V_{be3} - V_{be4} = 0. \quad (7)$$

The collector current of the transistor is given by

$$I_c = I_s \exp\left(\frac{V_{be}}{V_T}\right) \quad (8)$$

where the different terms have their usual meaning. Now, applying the translinear principle (TLP) [50] to Q_1 - Q_4 gives

$$I_{C1}I_{C2} = I_{C3}I_{C4}. \quad (9.1)$$

If $I_{C1} = I_i$, $I_{C2} = I_2$ and $I_{C4} = I_o$, then (9.1) becomes

$$I_i I_2 = I_{C3} I_o. \quad (9.2)$$

Collector current of Q_3 can be expressed as

$$I_{C3} = I_3 + C_1 \dot{V}_{C1}. \quad (10)$$

The derivative of the voltage across the capacitor C_1 is

$$\dot{V}_{C1} = \frac{dV_{C1}}{dt} = \frac{V_T}{I_o} \frac{dI_{out}}{dt} = \frac{V_T}{I_o} \dot{I}_o. \quad (11)$$

The derivative of the output current based on (8) yields

$$\dot{I}_o = \frac{dI_o}{dt} = \frac{I_s}{V_T} \exp\left(\frac{V_{C1}}{V_T}\right) \frac{dV_{C1}}{dt} = \frac{I_o}{V_T} \dot{V}_{C1}. \quad (12)$$

Substituting (10), (11) and (12) into (9), we get

$$I_i I_2 = \left(I_3 + \frac{C_1 \dot{I}_o V_T}{I_o} \right) I_o. \quad (13)$$

Suppose that we define the currents $I_2 = I_3 = I$, then (13) becomes

$$I_i = I_o + \frac{C_1 \dot{I}_o V_T}{I}. \quad (14)$$

By taking the Laplace transform into (14) and rearranging, the transfer function of the circuit of Fig. 3(a) in the s -domain is

$$H(s) = \frac{I_o(s)}{I_i(s)} = \frac{1}{s(C_1 V_T / I) + 1}. \quad (15)$$

It is seen from (15) that $H(s)$ corresponds to the transfer function of a lossy integrator, and that the natural frequency can be controlled by the bias current I .

Considering the direction of input and output currents in Fig. 3(a), it can be seen that this structure can easily produce the non-inverting lossy integrator function. The constant currents I_i , I_2 and I_3 are, respectively, replaced by

$I_{in} + I_B$, I_B and I_B as shown in Fig. 3(b). The current output I_{out} requires the bias current I_B for offset cancellation. The final current output of Fig. 3(b) is obtained as

$$\frac{I_{out}(s)}{I_a(s)} = \frac{-(I_B / C_1 V_T)}{s + (I_B / C_1 V_T)}. \quad (16)$$

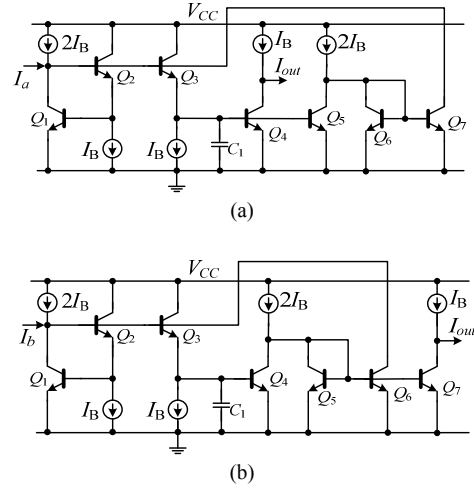


Fig. 4. Log-domain lossless integrator realized using a lossy integrator: (a) Inverting, (b) non-inverting.

As mentioned in Section 2.1, lossless integrator can be realized by feeding back the output current to the input. The inverting and non-inverting lossless integrators are, respectively, depicted in Fig. 4(a) and (b) and their transfer functions can be expressed as

$$\frac{I_{out}(s)}{I_a(s)} = \frac{-I_B}{s C_1 V_T}, \quad (17)$$

$$\frac{I_{out}(s)}{I_b(s)} = \frac{I_B}{s C_1 V_T}. \quad (18)$$

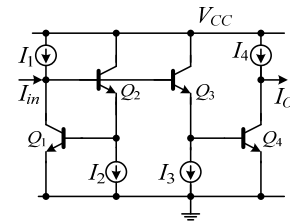


Fig. 5. Tunable translinear inverting current-gain.

2.4 Translinear Current-gain

The current-gain in this paper is facilitated by the translinear concept [49] as shown in Fig. 5, which provides the current output as a multiplier and divider. The bias currents are replaced and applied the input current (I_{in}) then the linear current output function can be obtained based on the translinear principle as

$$-\frac{I_2 I_{in}}{I_3} = -k I_{in} = I_o. \quad (19)$$

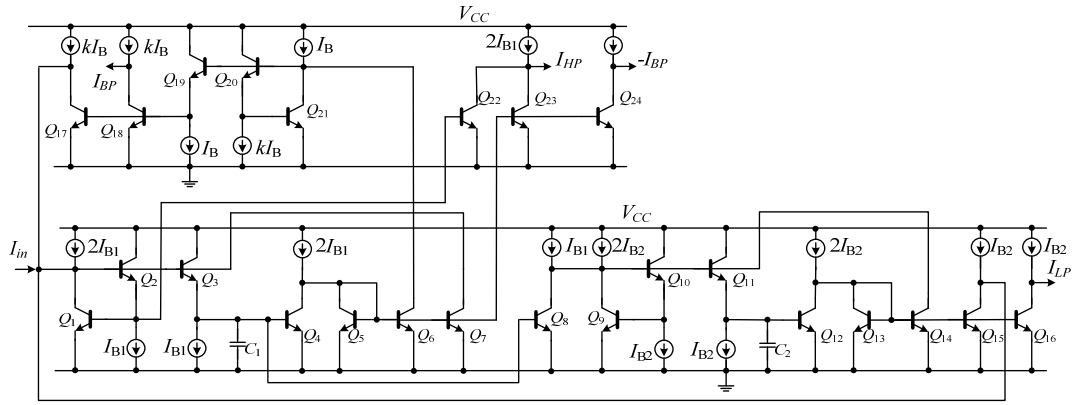


Fig. 6. Single-input multiple-output tunable log-domain current-mode universal filter.

It is found that the current gain can be adjusted by the ratio of bias currents I_2 and I_3 .

3. Log-domain Current-mode Universal Filter

The proposed filter as shown in Fig. 6 is realized based on the two-integrator loop structure, where the pole- Q is tunable by adjusting the current-gain block (k). It is straightforward to show that the output current of LP, BP and HP are given by

$$\frac{I_{LP}}{I_{in}} = \frac{-(I_{B1}I_{B2}/C_1C_2V_T^2)}{D(s)}, \quad (20)$$

$$\frac{I_{BP}}{I_{in}} = \frac{-s(kI_{B1}/C_1V_T)}{D(s)}, \quad (21)$$

$$\frac{I_{HP}}{I_{in}} = \frac{-s^2}{D(s)} \quad (22)$$

where $D(s) = s^2 + s(kI_{B1}/C_1V_T) + I_{B1}I_{B2}/C_1C_2V_T^2$.

Note that the proposed circuit can easily realize other two types of standard transfer functions by summing the particular outputs, which are summarized below.

- i) The BR response can be realized by summing of HP and LP output currents ($I_{HP} + I_{LP}$).
- ii) The AP response can be realized by summing of HP, LP and negative BP output currents ($I_{HP} + I_{LP} + (-I_{BP})$).

The pole-frequency (ω_0) and pole- Q (Q_0) can be expressed as

$$\omega_0 = \frac{1}{V_T} \sqrt{\frac{I_{B1}I_{B2}}{C_1C_2}}, \quad (23)$$

$$Q_0 = \frac{1}{k} \sqrt{\frac{I_{B2}C_1}{I_{B1}C_2}}. \quad (24)$$

The parameters I_{Bi} , V_T and k represent the bias currents, thermal voltage ($\approx 26\text{mV}$ at room temperature) and current-gain, respectively. From (23) and (24), it is seen that the pole-frequency can be linearly tuned by adjusting the bias currents (I_{Bi}), while the pole- Q can be electronically tuned by adjusting the current gain building block (k) without affecting the pole-frequency. Note that the pole-frequency is directly influenced by temperature (thermal voltage (V_T)). This effect can be reduced by using the compensated bias currents.

The current biasing circuit of the proposed filter is shown in Fig. 7, which is based on positive and negative

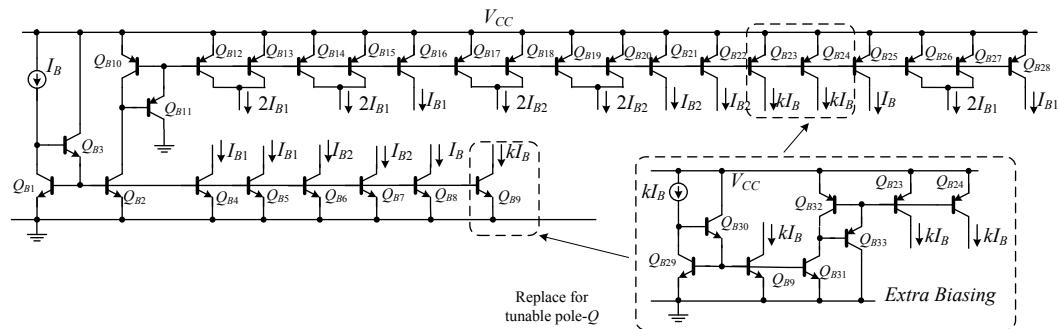


Fig. 7. Current biasing circuit based on simple current mirrors.

$$\frac{i_{out}(s)}{i_a(s)} \approx \frac{-g_{m2}g_{m3}g_{m4}r_{\pi1}r_{\pi2}r_{\pi3}r_{\pi4}r_{\pi7}}{g_{m1}g_{m2}g_{m3}r_{\pi1}r_{\pi2}r_{\pi3}r_{\pi4}r_{\pi7} - g_{m2}g_{m3}g_{m7}r_{\pi1}r_{\pi2}r_{\pi3}r_{\pi4}r_{\pi7} + s(g_{m1}g_{m2}r_{\pi1}r_{\pi2}r_{\pi3}r_{\pi4}r_{\pi7}C_1)}, \quad (25.1)$$

$$\frac{i_{out}(s)}{i_b(s)} \approx \frac{g_{m2}g_{m3}g_{m7}r_{\pi1}r_{\pi2}r_{\pi3}r_{\pi6}r_{\pi7}}{g_{m1}g_{m2}g_{m3}r_{\pi1}r_{\pi2}r_{\pi3}r_{\pi6}r_{\pi7} - g_{m2}g_{m3}g_{m6}r_{\pi1}r_{\pi2}r_{\pi3}r_{\pi6}r_{\pi7} + s(g_{m1}g_{m2}r_{\pi1}r_{\pi2}r_{\pi3}r_{\pi6}r_{\pi7}C_1)}. \quad (25.2)$$

current mirrors. For $Q_0 = 1$, the positive and negative bias currents can be tuned simultaneously by single bias current I_B . The general current biasing circuit contains transistors Q_{B1} – Q_{B28} that are implemented to the 18 bias currents. For tunable pole- Q , Q_{B9} , Q_{B23} , Q_{B24} are removed and replaced by the extra biasing circuit. Pole- Q can be independently tuned by adjusting the extra bias current kI_B and the pole-frequency is tuned by bias current I_B .

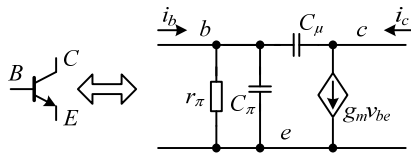


Fig. 8. Simple small signal of BJT transistor.

4. Non-idealities Studies

Log-domain filter suffers from transistor nonidealities. The study of nonideal log-domain filters is complicated in the fact that the non-linear logarithmic-exponential operations inherent the circuit result in transcendental equations. This paper derives equations describing the non-ideal characteristics of the log-domain circuit as a consequence of the deviations in the nonideal parameters. This section shows the effects of the transistor parasitic in Fig. 8 based on a small-signal model using transconductance ($g_m = I_C / V_T$), base-emitter resistance (r_{π}), base-emitter capacitance (C_{π}), and base-collector capacitance (C_{μ}). We assume that the other parasitic capacitances are very small and the impedance of the collector-emitter (r_{ce}) is high. Physical parameters such as area mismatch and early voltage are also discussed.

4.1 Influences of Parasitic Resistance (r_{π})

This qualitative analysis shows that the transistor non-idealities, including the parasitic resistances and parasitic capacitances, are the sources of error within log-domain circuits. Finite beta and base-emitter resistance have generally been identified as the most problematic error sources at low frequencies [51].

$$\frac{i_{out}(s)}{i_a(s)} \approx \frac{-g_{m2}g_{m3}g_{m4}}{g_{m1}g_{m2}g_{m3} - g_{m2}g_{m3}g_{m7} + s[g_{m1}g_{m2}(C_1 + C_{\pi3} + C_{\pi7} + C_{\pi4}) + g_{m1}g_{m3}C_{\pi2} - g_{m2}g_{m7}C_{\pi3} - g_{m3}g_{m7}(C_{\pi2} + C_{\pi1})]}, \quad (27.1)$$

$$\frac{i_{out}(s)}{i_b(s)} \approx \frac{-g_{m2}g_{m3}g_{m4}}{g_{m1}g_{m2}g_{m3} - g_{m2}g_{m3}g_{m7} + s[g_{m1}g_{m2}(C_1 + C_{\mu7} + C_{\mu4}) + g_{m1}g_{m3}C_{\mu1} + g_{m2}g_{m3}(C_{\mu2} + C_{\mu3} + C_{\mu7}) - g_{m3}g_{m7}C_{\mu1}]}, \quad (27.2)$$

Parasitic base-emitter resistance (r_{π}) is a limitation of the translinear circuit accuracy at high-frequencies. From the small-signal model of a bipolar transistor, when the parasitic capacitances are neglected, the effect of r_{π} to inverting and non-inverting lossless integrator transfer function is, respectively, described by (25.1) and (25.2). They can be simplified and rewritten as

$$\frac{i_{out}(s)}{i_a(s)} \approx \frac{-g_{m2}g_{m3}g_{m4}}{g_{m1}g_{m2}g_{m3} - g_{m2}g_{m3}g_{m7} + s(g_{m1}g_{m2}C_1)}, \quad (26.1)$$

$$\frac{i_{out}(s)}{i_b(s)} \approx \frac{g_{m2}g_{m3}g_{m7}}{g_{m1}g_{m2}g_{m3} - g_{m2}g_{m3}g_{m6} + s(g_{m1}g_{m2}C_1)}. \quad (26.2)$$

From (26), it can be seen that the both types of lossless integrators has no effects from the parasitic resistance (r_{π}). Moreover, it can be seen that the transistor Q_1 and Q_7 should be matched for inverting lossless in integrator. Likewise, the transistor Q_1 and Q_6 should be matched for inverting lossless in integrator. The function of lossless integrators can be well operated according to the theoretical aspect.

4.2 Influences of Parasitic Capacitance (C_{π} and C_{μ})

Parasitic base-emitter capacitance (C_{π}) is also a major limitation to translinear circuit accuracy, particularly at high-frequencies. Using the small-signal model of the bipolar transistor with parasitic capacitances, the effect of C_{π} to inverting lossless integrator transfer function can be approximated in (27.1) and (27.2).

Assuming that the transconductances of the transistors are matched, the transfer functions in (27.1) and (27.2) become

$$\frac{i_{out}(s)}{i_a(s)} \approx \frac{-g_m}{s(C_1 + C_{\pi7} + C_{\pi4} - C_{\pi1})}, \quad (28.1)$$

$$\frac{i_{out}(s)}{i_b(s)} \approx \frac{-g_m}{s(C_1 + 2C_{\mu7} + C_{\mu4} + C_{\mu2} + C_{\mu3})}. \quad (28.2)$$

$$\frac{i_{out}(s)}{i_b(s)} \approx \frac{g_{m2}g_{m3}g_{m7}}{g_{m1}g_{m2}g_{m3} - g_{m2}g_{m3}g_{m6} + s[g_{m1}g_{m2}(C_1 + C_{\pi3} + C_{\pi6} + C_{\pi7}) + g_{m1}g_{m3}C_{\pi2} - g_{m2}g_{m6}C_{\pi3} - g_{m3}g_{m6}(C_{\pi1} + C_{\pi2})]}, \quad (29.1)$$

$$\frac{i_{out}(s)}{i_b(s)} \approx \frac{g_{m2}g_{m3}g_{m7}}{g_{m1}g_{m2}g_{m3} - g_{m2}g_{m3}g_{m6} + s[g_{m1}g_{m2}(C_1 + C_{\mu7} + C_{\mu6}) + g_{m1}g_{m3}C_{\mu1} - g_{m3}g_{m6}C_{\mu1} + g_{m2}g_{m3}(C_{\mu2} + C_{\mu3} + C_{\mu6})]}. \quad (29.2)$$

Similarly, parasitic base-collector capacitance (C_{μ}) is also a major limitation to translinear circuit accuracy. The effect of the base-collector capacitance to the non-inverting lossless integrator transfer function is given by (29.1) and (29.2).

Again assuming that the transconductances of the transistors are matched, the transfer functions in (29.1) and (29.2) become

$$\frac{i_{out}(s)}{i_b(s)} \approx \frac{g_m}{s(C_1 + C_{\pi6} + C_{\pi7} - C_{\pi1})}, \quad (30.1)$$

$$\frac{i_{out}(s)}{i_b(s)} \approx \frac{g_m}{s(C_1 + C_{\mu2} + C_{\mu3} + C_{\mu7} + 2C_{\mu6})}. \quad (30.2)$$

From (30.1) and (30.2), it is seen that the parasitic capacitances C_{π} and C_{μ} produce a small deviation in the frequency response in lossless integrators. The natural frequency is of the form $\omega_0 = I / CV_T$, high frequency operation can be realized by increasing the bias current or reducing the capacitance. To maintain the low-power, the bias currents are kept at a lower level and the integrating capacitance is increased. To prevent significant distortion, the selected capacitance C should be

$$C \gg C_{\pi i} + 5C_{\mu i}. \quad (31)$$

Note that there are high-order poles (2nd and 3rd order poles) which affect to higher frequencies than the operation frequency of the filter. These poles can be neglected.

4.3 Influences of Area Mismatches

Emitter area mismatches cause variations in the saturation current (I_S) between transistors. Taking into account the emitter area, (14) can be rewritten as

$$\lambda k I_{in} = I_{out} + \frac{C_1 \dot{I}_{out} V_T}{I} \quad (32)$$

$$\text{where } \lambda = \frac{I_{S3}I_{S4}}{I_{S1}I_{S2}} = \frac{A_3A_4}{A_1A_2}.$$

From (32), it is clear that the area mismatches introduce only a change in the proportionality constant or DC gain of the low-pass filter without affecting the linearity or the time constant of the circuit. The gain error can be easily compensated by adjusting one of the DC bias currents.

4.4 Influences of Early Effect

Early effect (base-width modulation) causes the collector current error by the collector-emitter and base-col-

lector voltages. Considering the variation of collector-emitter voltage, the collector current can be written as $I_c = (1 + V_{ce}/V_A)I_S \exp(V_{be}/V_T)$, where V_A is the forward-biased early voltage. An analysis of the integrator shows the early effect with a scalar error to the DC gain of the circuit as in the case of the area mismatches. Since V_{ce} has been signal-dependent, the device base-width modulation also introduces distortion. Since the voltage swings in the current-mode companding circuits have been very low (δV_{bes}), the early effect is not a major source of distortion.

4.5 Influences of the Bias Currents

The proposed log-domain filter employs bias currents which are provided by positive and negative current sources. The positive (I_{BP}) and negative (I_{BN}) current sources are respectively replaced by positive and negative current mirrors in Fig. 7. The transconductance of the transistors are controlled by the particular bias currents. Positive and negative current mirror errors which affect the filter performances are considered.

Based on the configuration of lossless integrators in Fig. 4, the positive and negative bias currents are given by $I_{BP} = \alpha_P I_B$ and $I_{BN} = \alpha_N I_B$, where α_P and α_N represent the current gains of the positive and negative current mirrors, respectively. It can be seen that if the transconductances $g_{m1} = g_{m4} = g_{m5} = g_{m6} = g_{m7} = g_{mp}$ and $g_{m2} = g_{m3} = g_{mn}$, then (26.1) and (26.2) become

$$\frac{i_{out}(s)}{i_a(s)} \approx \frac{-g_{mn}}{sC_1} = \frac{-\alpha_N I_B}{sV_T C_1}, \quad (33.1)$$

$$\frac{i_{out}(s)}{i_b(s)} \approx \frac{g_{mn}}{sC_1} = \frac{\alpha_N I_B}{sV_T C_1}. \quad (33.2)$$

From the translinear current gain in Fig. 5, current output has no effects from the current gain of current mirrors. It can be seen that the gain of current mirrors affect only the lossless integrator configurations. Re-analyzing Fig. 6, the denominator can be rewritten as

$$D_n(s) = s^2 + s(\alpha_N k I_B / C_1 V_T) + \alpha_N^2 I_B^2 / C_1 C_2 V_T^2. \quad (34)$$

The non-ideal pole-frequency (ω_{0n}) and pole- Q (Q_{0n}) can be expressed as

$$\omega_{0n} = \frac{\alpha_N I_B}{V_T} \sqrt{\frac{1}{C_1 C_2}}, \quad (35)$$

$$Q_{0n} = \frac{1}{k} \sqrt{\frac{C_1}{C_2}}. \quad (36)$$

It is evident from (35) that slight deviation only in the pole-frequency is caused due to the errors of the bias current I_{BN} . To reduce these errors, accurate current mirrors as well as cascode current mirrors are required. Note that the pole- Q has no effects from the error of bias currents.

```

.MODEL C12TYP NPN
+ (IS=7.40E-018 BF=1.00E+002 BR=1.00E+000 NF=1.00E+000
+ NR=1.00E+000 TF=6.00E-012 TR=1.00E-008 XTF=1.00E+001
+ VTF=1.50E+000 ITF=2.30E-002 PTF=3.75E+001 VAF=4.50E+001
+ VAR=3.00E+000 IKF=3.10E-002 IKR=3.80E-003 ISE=2.80E-016
+ NE=2.00E+000 ISC=1.50E-016 NC=1.50E+000 RE=5.26E+000
+ RB=5.58E+001 IRB=0.00E+000 RBM=1.55E+001 RC=8.09E+001
+ CJE=3.21E-014 VJE=1.05E+000 MJE=1.60E-001 CJC=2.37E-014
+ VJC=8.60E-001 MJC=3.40E-001 XCJC=2.30E-001 CJS=1.95E-014
+ VJS=8.20E-001 MJS=3.20E-001 EG=1.17E+000 XTB=1.70E+000
+ XTI=3.00E+000 KF=0.00E+000 AF=1.00E+000 FC=5.00E-001)

```

(a) NPN-HSB2 provided by ST Microelectronics

```

.model HFA3128 PNP
+ (IS=1.027E-16 XTI=3.000E+00 EG=1.110E+00 VAF=3.000E+01
+ VAR=4.500E+00 BF=5.228E+01 ISE=9.398E-20 NE=1.400E+00
+ IKF=5.412E-02 XTB=0.000E+00 BR=7.000E+00 ISC=1.027E-14
+ NC=1.800E+00 IKR=5.412E-02 RC=3.420E+01 CJC=4.951E-13
+ MJC=3.000E-01 VJC=1.230E+00 FC=5.000E-01 CJE=2.927E-13
+ MJE=5.700E-01 VJE=8.800E-01 TR=4.000E-09 TF=20.05E-12
+ ITF=2.001E-02 XTF=1.534E+00 VTF=1.800E+00 PTF=0.000E+00
+ XCJC=9.000E-01 CJS=1.150E-13 VJS=7.500E-01 MJS=0.000E+00
+ RE=1.848E+00 RB=3

```

(b) PNP-HFA3128 provided by Intersil

Tab. 1. Bipolar model parameter of used for SPICE simulation.

5. Simulation Results

In order to verify the operation of the circuit topology of Fig. 6, a filter with a single input and four outputs is designed. The power supply voltage (V_{CC}) is assigned to 2.5 V and the bias current I_B is varied from 0.01 μA to 1,000 μA at room temperature. To prevent the parasitic effects of the filter, capacitors are chosen to be much larger than $C_\pi + 5C_\mu$ by assigning $C_1 = C_2 = 50$ pF. The high-speed bipolar technology (HSB2) provided by ST Microelectronics [52] is used in the simulations. The transistor model is listed in Tab. 1.

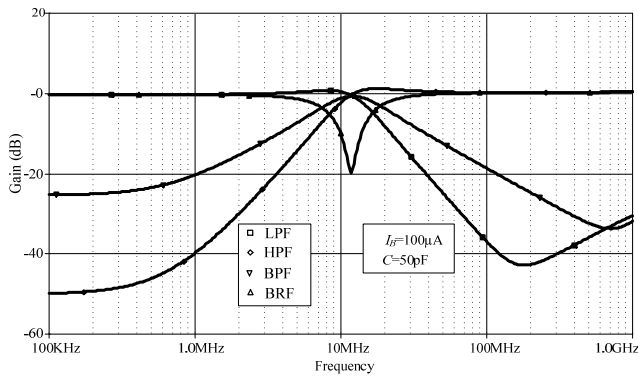


Fig. 9. LP, HP and BP filter characteristics at $I_B = 100 \mu\text{A}$, $C = 50$ pF.

The amplitude response of LP, BP, HP and BR filters based on Fig. 6 with $I_B = 100 \mu\text{A}$ and $C_1 = C_2 = 50$ pF is shown in Fig. 9. Fig. 10 illustrates amplitude and phase responses simulation around 10 MHz of AP filter.

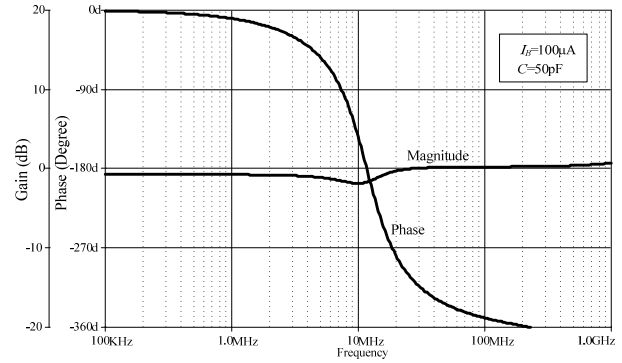


Fig. 10. AP filter characteristics.

Fig. 11 shows the tunable pole-frequency of BP filter by varying the current bias (I_B) from 0.01 μA to 1,000 μA . A wide range of pole-frequency tuning is obtained from 1 kHz to 100 MHz.

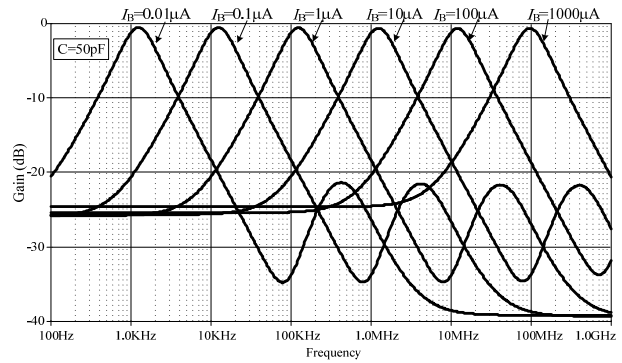


Fig. 11. Tunable BP frequency response by using various bias currents.

A comparison of the magnitude response between the simulated LP filter and the ideal Butterworth LP function in (20) is exhibited in Fig. 12. Slight difference in frequency responses of simulated and ideal LP functions is observed due to the effects of parasitic capacitances at high frequency which was discussed in Section 4.2.

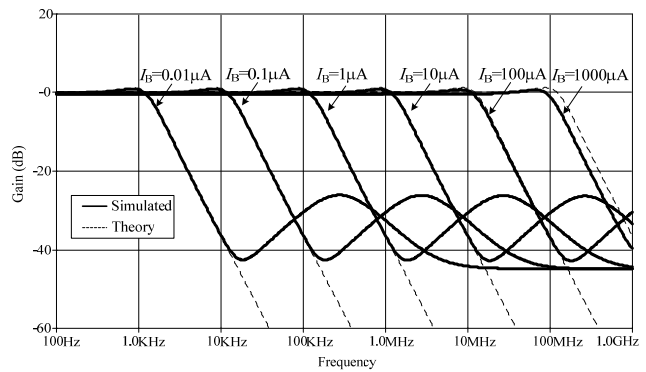


Fig. 12. Comparison between the simulation results and theoretical results.

The pole- Q can be electronically tuned (at 10 MHz) from 1 to 16 by assigning $I_B = 100 \mu\text{A}$ and varying the current bias kI_B from $6.25 \mu\text{A}$ to $100 \mu\text{A}$, and is shown in Fig. 13.

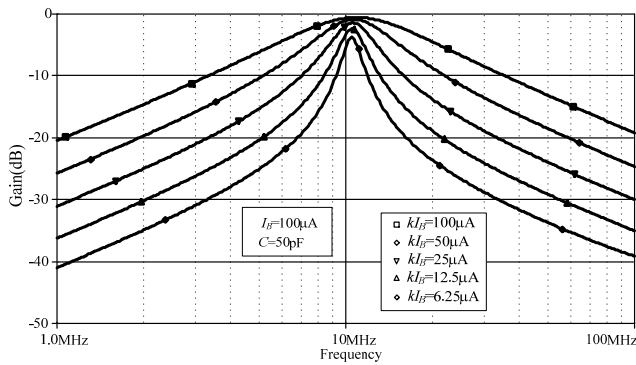


Fig. 13. Pole- Q tuning characteristics for $Q = 1, 2, 4, 8$ and 16 .

Frequency response of the proposed filter for a time-domain signal can be investigated by assigning the BP pole-frequency at 100 MHz ($I_B = 1,000 \mu\text{A}$). The different frequencies of sinusoidal input (10 MHz, 100 MHz and 1 GHz) are applied based on $200 \mu\text{A}$ -p. The linear tunability range of frequency response from 1 kHz to 100 MHz based on various bias currents from $0.01 \mu\text{A}$ to $1,000 \mu\text{A}$ and $C = 50 \text{ pF}$ is illustrated in Fig. 14.

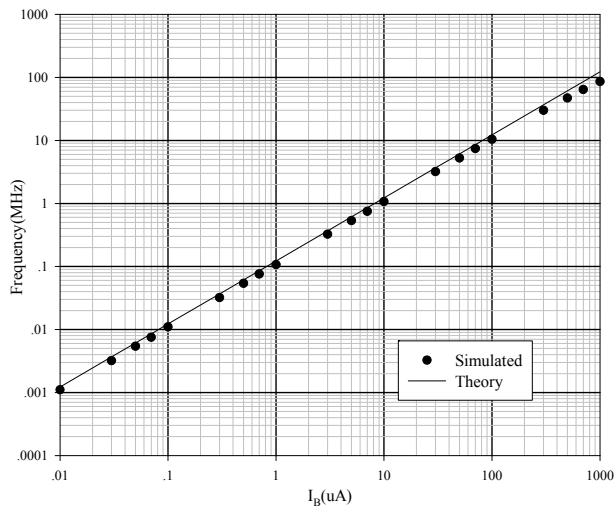


Fig. 14. Tunable frequency response by using various bias currents.

The different frequency output currents of BP filter ($f_0 = 100 \text{ MHz}$) are shown in Fig. 15(a)-(c). It can be seen that the highest current output (Fig. 15(b)) is obtained at 100 MHz.

Noise analysis at different outputs of the proposed filter is shown in Fig. 16. Low-noise values of LP, BP and HP filters are obtained lower than $133 \text{ pV}/\sqrt{\text{Hz}}$.

Tab. 2 illustrates a comparison of the proposed universal filter with previous universal filters. The first 2 papers are based on log-domain concept [16], [17]. The rest [27], [35], [36], [38], [41] and [43] are based on different active building blocks (ABB). Note that the existing universal filters have at least drawbacks of requiring dual sup-

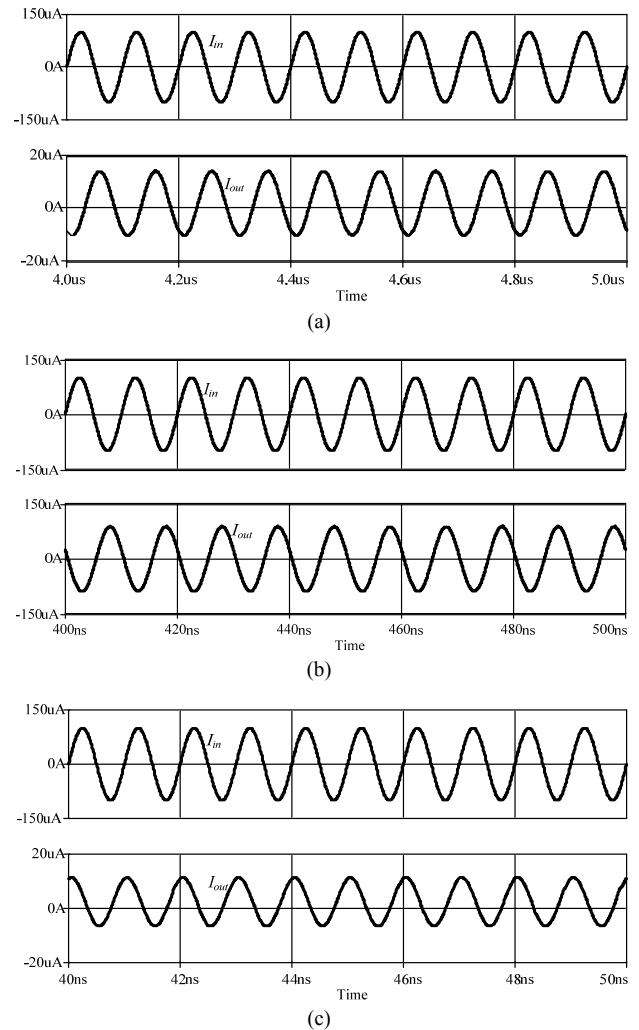


Fig. 15. Time domain response of BP filter based on $f_0 = 100 \text{ MHz}$: (a) input = 10 MHz, (b) input = 100 MHz, (c) input = 1 GHz.

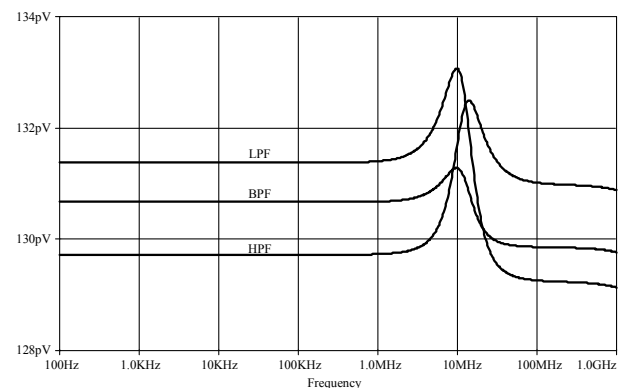


Fig. 16. Noise analysis of proposed filter based on $f_0 = 10 \text{ MHz}$.

plies and many transistors. Although, the class-AB log-domain filter [16] provides quite good performance in frequency response but suffers by many transistors, four capacitors, current splitter and complex structure. Another log-domain SIMO and MISO filters [17] use low power supply but suffer by high number of components (BJT and MOS), extra voltage sources and complex structure. The ABB-based filters [27], [35], [36], [38], [41] and [43] can

operate only in low megahertz range with narrow tunable ranges. The proposed filter based on +2.5 V single supply offers the following features: high frequency, linear wide-range tunability, simply structure and low-component count.

Filter	Power supply	Tunable frequency range	Number of transistors	Use of resistor	Mode of operation
[16]	+3 V	149 MHz	47	No	CM
[17]	+1.5 V	10 MHz	58/52	No	CM
[27]	± 5 V	< 10 MHz	47	No	CM
[35]	± 2.5 V	< 22.5 MHz	62	No	CM
[36]	± 1.25 V	< 10 MHz	36	Yes	VM
[38]	± 2.5 V	< 10 MHz	56	No	CM
[41]	± 1.25 V	< 10 MHz	70	No	CM
[43]	± 2.5 V	< 5 MHz	98	No	CM/VM
Proposed	+2.5 V	1k-100 MHz	24	No	CM

Tab.2. Comparison of previous universal filters with the proposed filter. (Remark: Some preliminary results of the paper have appeared in [20].)

6. Conclusion

A novel low-voltage single-input multiple-output current-mode universal filter based on log-domain concept has been presented. The proposed filter is realized based on two lossless integrators loop concept which consists of two lossless integrator, a current gain and additional transistors for obtaining outputs. Each lossless integrator contains only 7 transistors and a grounded capacitor which is realized by transforming a lossy integrator. Five types of standard filter functions with high impedance output currents are produced based on a 2.5 V power supply. The proposed filter consists of 24 transistors and 2 grounded capacitors. A wide range of tunable pole-frequency is obtained from 1 kHz to 100 MHz by varying I_B from 0.01 μ A to 1000 μ A. The pole- Q can be tuned without affecting the pole-frequency.

Acknowledgement

The authors would like to express their sincere thanks to Dr. M.N.S. Swamy of Concordia University, Canada and Mr. Natapong Wongprommoon and anonymous reviewers for their very helpful comments and suggestions, which have significantly improved the manuscript.

References

[1] ADAMS, R. W. Filtering in the log domain. In *63rd AES Conv.* Los Angeles (CA), May 1979, preprint 1470.

[2] FREY, D. R. Log-domain filtering: An approach to current-mode filtering. *Proc. IEE, part G*, 1993, vol. 140, no. 6, p. 406–416.

[3] FREY, D. R. Exponential state-space filters: a generic current mode design strategy. *IEEE Trans Circuits Systems-I*, 1996, vol. 43, p. 34–42.

[4] SEEVINCK, E. Companding current-mode integrator: A new circuit principle for continuous-time monolithic filters. *Electron. Lett.*, 1990, vol. 26, no. 24, p. 2046–2047.

[5] TSIVIDIS, Y. On linear integrators and differentiators using instantaneous companding. *IEEE Trans. Circuits Syst. II*, Aug. 1995, vol. 42, p. 561–564.

[6] TSIVIDIS, Y. General approach to signal processors employing companding. *Electron. Lett.*, 1995, vol. 31, no. 18, p. 1549–1550.

[7] TSIVIDIS, Y. Instantaneously companding integrators. In *Proc. IEEE Int. Symp. Circuits Syst. (ISCAS'97)*. Hong-Kong, 1997, vol. 1, p. 477–480.

[8] FREY, D. R. A 3.3 V electronically tunable active filter usable to beyond 1 GHz. In *Proc. IEEE Int. Symp. Circuits Syst. (ISCAS'94)*. London (U.K.), 1994, vol. 5, p. 493–496.

[9] FREY, D. R. On log-domain filtering for RF applications. *IEEE J. Solid-State Circuits*, Oct. 1996, vol. 31, p. 1468–1475.

[10] FREY, D. R. An adaptive analog notch filter using log-filtering. In *Proc. IEEE Int. Symp. Circuits Syst. (ISCAS'96)*. Atlanta (GA), 1996, vol. 1, p. 297–300.

[11] KIRCA, A., CAM, U. A novel log-domain first-order multifunction filter. *ETRI Journal*, June 2006, vol. 28, no. 3.

[12] DRAKAKIS, E. M., PAYNE, A. J., TOUMAZOU, C. Log-domain filtering and the Bernoulli cell. *IEEE Trans. Circuits Syst. I*, May 1999, vol. 46, no. 5, p. 559–571.

[13] PSYCHALINOS, C. On the transposition of Gm-C filters to DC stabilized log-domain filters. *Int. J. Circ. Theor. Appl.*, 2006, no. 34, p. 217–236.

[14] PSYCHALINOS, C. Realization of log-domain high-order transfer functions using first-order building blocks and complementary operators. *Int. J. Circ. Theor. Appl.*, 2007, vol. 35, p. 17–32.

[15] PSYCHALINOS, C. Log-domain linear transformation filters revised- improved building blocks and comparison results. *Int. J. Circ. Theor. Appl.*, 2008, vol. 36, p. 119–133.

[16] TOLA, A. T., ARSLANALP, R., YILMAZ, S. S. Current mode high-frequency KHN filter employing differential class AB log domain integrator. *International Journal of Electronics and Communications (AEÜ)*, 2009, vol. 63, no. 7, p. 600–608.

[17] PSYCHALINOS, C. Log-domain SIMO and MISO low-voltage universal biquads. *Analog Integrated Circuits and Signal Processing*, 2011, vol. 67, no. 2, p. 201–211.

[18] PROMMEE, P., SRA-IUM, N., DEJHAN, K. High-frequency log-domain current-mode multiphase sinusoidal oscillator. *IET Circuits Devices Syst.*, 2010, vol. 4, no. 5, p. 440–448.

[19] PROMMEE, P., PRAPAKORN, N., SWAMY, M.N.S. Log-domain current-mode quadrature sinusoidal oscillator. *Radioengineering*, 2011, vol. 20, no.3, p. 600–607.

[20] PROMMEE, P., SOMDUNYAKANOK, M., ANGKEAW, K., DEJHAN, K. Tunable current-mode log-domain universal filter. In *Proc. of IEEE ISCAS 2010*. Paris (France), May 29–June 2, 2010.

[21] KERWIN, W. J., HUELSMAN, L. P., NEWCOMB, R. W. State-variable synthesis for insensitive integrated circuit transfer function. *IEEE Trans. Solid-state Circuits*, 1967, vol. SC-2, p. 87–92.

[22] SANCHEZ-SINENCIO, E., GEIGER, R. L., NEVAREZ-LOZANO, H. Generation of continuous-time two integrator loop OTA

- filter structures. *IEEE Trans. Circuits and Syst.*, 1988, vol. 35, p. 936-946.
- [23] WU, J., XIE, C. New multifunction active filter. *Int. J. Electron.*, 1993, vol. 74, p. 235-239.
- [24] CHANG, C. New multifunction OTA-C biquads. *IEEE Trans. Circuits and Syst.*, 1999, vol. 46, p. 820-824.
- [25] CHANG, C., PAI, S. Universal current-mode OTA-C biquad with the minimum components. *IEEE Trans. Circuits and Syst.*, 2000, vol. 47, p. 1235-1238.
- [26] CHANG, C., AL-HASHIMI, B. M., ROSS, J. N. Unified active filter biquad structure. *IEE Proc., part G*, 2004, vol. 151, p. 273-277.
- [27] PROMMEE, P., PATTANADAPONG, T. Realization of tunable pole-Q current-mode OTA-C universal filter. *Circuits, Systems, and Signal Processing*, Oct. 2010, vol. 29, no. 5.
- [28] SUN, Y., FIDLER, J. K. Structure generation of current-mode two integrator loop dual output-OTA grounded capacitor filters. *IEEE Trans. Circuits and Syst.*, 1996, vol. 43, p. 659-663.
- [29] CHANG, C., AL-HASHIMI, B. M. Analytical synthesis of current-mode high-order OTA-C filters. *IEEE Trans. Circuits and Syst.*, 2003, vol. 50, p. 1188-1192.
- [30] TU, S. H., CHANG, C., ROSS, J. N., SWAMY, M. N. S. Analytical synthesis of current-mode high-order single-ended-input OTA and equal-capacitor elliptic filter structures with the minimum number of components. *IEEE Trans. Circuits and Syst. I*, 2007, vol. 54, p. 2195-2210.
- [31] AL-HASHIMI, B. M., DUDEK, F., MONIRI, M., LIVING, J. Integrated universal biquad based on triple-output OTAs and using digitally programmable zeros. *IEE Proc., part G*, 1998, vol. 145, p. 192-196.
- [32] WANG, H. Y., LEE, C. T. Versatile insensitive current-mode universal biquad implementation using current conveyors. *IEEE Trans. Circuits and Syst. II*, 2001, vol. 48, p. 409-413.
- [33] YUCE, E., MINAEI, S. Signal limitations of the current-mode filters employing current conveyors. *Internat. Journal of Electronics and Communications (AEÜ)*, 2008, vol. 62, p. 193-198.
- [34] HORNG, J. W., HOU, C. L., CHANG, C. M., CHIU, W.-Y., LIU, C.-C. Current-mode universal biquadratic filter with five inputs and two outputs using two multi-output CCII's. *Circuits Systems and Signal Processing*, 2009, vol. 28, p. 781-792.
- [35] IBRAHIM, M. A., MINAEI, S., KUNTMAN, H. A 22.5 MHz current-mode KHN-biquad using differential voltage current conveyor and grounded passive elements. *Internat. Journal of Electronics and Communications (AEÜ)*, 2005, vol. 59, p. 311-318.
- [36] HORNG, J. W. High input impedance voltage-mode universal biquadratic filter with three inputs using DDCCs. *Circuits Systems and Signal Processing*, 2008, vol. 27, p. 553-562.
- [37] FABRE, A., SAAID, O., WIEST, F., BOUCHERON, C. Low power current-mode second-order bandpass IF filter. *IEEE Trans. Circuits and Syst. II*, 1997, vol. 44, p. 436-446.
- [38] YUCE, E., MINAEI, S., CICEKOGLU, O. Universal current-mode active-C filter employing minimum number of passive elements. *Analog Integrated Circuits and Signal Processing*, 2006, vol. 46, no. 2, p. 169-171.
- [39] YUCE, E., TOKAT, S., MINAEI, S., CICEKOGLU, O. Stability problems in universal current-mode filters. *Int. Journal of Electronics and Communications (AEÜ)*, 2007, vol. 61, p. 580 - 588.
- [40] YUCE, E., MINAEI, S. On the realization of high-order current-mode filter employing current controlled conveyors. *Computer and Electrical Engineering Journal*, 2008, vol. 34, p. 165-172.
- [41] MINAEI, S. Electronically tunable current-mode universal biquad filter using dual-X current conveyors. *Journal of Circuits, Systems, and Computers*, 2009, vol. 18, no. 4, p. 665-680.
- [42] TSUKUTANI, T., HIGASHIMURA, M., SUMI, Y., FUKUI, Y. Electronically tunable current-mode active-only biquadratic filter. *International Journal of Electronics*, 2000, vol. 87, p. 307-314.
- [43] MINAEI, S., CICEKOGLU, O., KUNTMAN, H., DUNDAR, G., CERID, O. New realizations of current-mode and voltage-mode multifunction filters without external passive elements. *International Journal of Electronics and Communications (AEÜ)*, 2003, vol. 57, p. 63-69.
- [44] KHORRAMABADI, H., GRAY, P. R. High frequency CMOS continuous-time filters. *IEEE J. Solid-State Circuits*, Dec. 1984, vol. SC-19, no. 6, p. 939-948.
- [45] GOPINATHAN, V., TSIVIDIS, Y. P., TAN, K. S., HESTER, R. K. Design considerations for high-frequency continuous-time filters and implementation of an antialiasing filter for digital video. *IEEE J. Solid-State Circuits*, Dec. 1990, vol. 25, no. 6, p. 1368-1378.
- [46] SNELGROVE, W. M., SHOVAL, A. A balanced 0.9- μ m CMOS transconductance-C filter tunable over the VHF range. *IEEE J. Solid-State Circuits*, Mar. 1992, vol. 27, no. 3, p. 314-323.
- [47] NAUTA, B. A CMOS transconductance-C filter technique for very high frequencies. *IEEE J. Solid-State Circuits*, Feb. 1992, vol. 27, no. 2, p. 142-153.
- [48] KHOURY, J. M. Design of a 15-MHz CMOS continuous-time filter with on-chip tuning. *IEEE J. Solid-State Circuits*, Dec. 1991, vol. 25, no. 12, p. 1988-1997.
- [49] TOUMAZOU, C., LIDGEY, F. J., HAIGH, D. G. *Analog IC Design: The Current-mode Approach*. London (UK): Peter Peregrinus Ltd., 1990.
- [50] GILBERT, B. Translinear circuits: a historical overview. *Analog Integrated Circuits and Signal Processing*, Mar. 1996, vol. 9, no. 2, p. 95-118.
- [51] LEUNG, V. W., ROBERTS, G. W. Effects of transistor nonidealities on high-order log-domain ladder filter pole-frequencies. *IEEE Trans. Circuits Syst. II*, May 2000, vol. 47, no. 5, p. 373-387.
- [52] ALIOTO, M., PALUMBO, C. *Model and Design of Bipolar and MOS Current-mode Logic: CML, ECL and SCL Digital Circuits*. Dordrecht (Netherlands): Springer, 2005.

About Authors

Pipat PROMMEE received his B.Ind. Tech. degree in Telecommunications, M.Eng. and D.Eng. in Electrical Engineering from Faculty of Engineering, King Mongkut's Institute of Technology Ladkrabang (KMITL), Bangkok, Thailand in 1992, 1995 and 2002, respectively. He was a senior engineer of CAT telecom plc. between 1992 and 2003. Since 2003, he has been a faculty member of KMITL. He is currently an associate professor at the Telecommunications Engineering Department at KMITL. He is author or co-author of more than 60 publications in journals and proceedings of international conferences. His research interests are focusing in analog signal processing, analog filter design and CMOS analog integrated circuit design. He is a member of IEEE, USA.

Kobchai DEJHAN received the B.Eng. and M.Eng. degree in Electrical Engineering from King Mongkut's Institute of Technology Ladkrabang (KMITL), Bangkok, Thailand, in 1978 and 1980, respectively and Doctor

degree in Telecommunication from Ecole Nationale Supérieure des Telecommunications (ENST) Paris, France (Telecom Paris) in 1989. Since 1980, he has been a member of the Department of Telecommunication at Faculty of Engineering, KMITL, where he is currently an associate

professor of telecommunication. His research interests include analog circuit design, digital circuit design and telecommunications circuit design and systems include analog circuit design, digital circuit design and telecommunication circuit design and systems.